ISSN 1067-8212, Russian Journal of Non-Ferrous Metals, 2018, Vol. 59, No. 2, pp. 181–189. © Allerton Press, Inc., 2018.
Original Russian Text © A.M. Mamonov, S.S. Slezov, O.N. Gvozdeva, 2018, published in Izvestiya Vysshikh Uchebnykh Zavedenii, Tsvetnaya Metallurgiya, 2018, No. 1, pp. 53–63.

PHYSICAL METALLURGY AND HEAT TREATMENT

Controlling the Phase Composition, Structure, and Complex of Properties of the High-Modulus Titanium Alloy by Thermohydrogen Processing

A. M. Mamonov*, S. S. Slezov, and O. N. Gvozdeva*****

Moscow Aviation Institute (National Research University), Moscow, 121552 Russia

**e-mail: mitom@implants.ru*

***e-mail: slezov93@mail.ru*

****e-mail: gon7133@mail.ru*

Received March 21, 2017; in final form, May 19, 2017; accepted for publication September 29, 2017

Abstract—The possibilities and efficiency of applying the thermohydrogen processing (THP) of the high-modulus Ti–8.7Al–1.5Zr–2.0Mo titanium alloy with an aluminum content exceeding the solubility limit in α-titanium are considered. Experimental data on the influence of hydrogen on the alloy phase composition and structure are acquired. Regularities of phase transformations in the hydrogen-containing alloy under various thermal impacts are analyzed. The phase diagram of the alloy–hydrogen system in the hydrogen concentration range from the initial one to 1.0 wt % and the temperature range from 20 to 1100°C is constructed. It is shown that a single-phased β-structure is fixed with the concentration of introduced hydrogen of 0.6 wt % and higher by means of quenching from the β-region. Hydrogen saturation up to 0.8–1.0% leads to the implementation of the $\beta \rightarrow \delta$ shear hydride transformation during quenching from temperatures below 750°C, and to the partial eutectoid transformation of the β-phase under slow cooling. It is established that hydrogen extends the stability region of the β-phase, lowering the temperature of the $\beta/(\alpha + \beta)$ transition by 210°C (at 1.0% H), and increases the stability temperature of the α_2-phase by 50°C. The process flowsheets and THP modes forming two structural types—submicrocrystalline and bimodal—are developed and approved for alloy samples. The formation mechanisms of these structures during THP are analyzed and the mechanical properties of the alloy are determined. It is established that THP leads to an increase in strength and hardness when compared with the initial state. The THP forming the microcrystalline structure causes a decrease in plasticity characteristics at the maximal hardness.

Keywords: titanium alloy, hydrogen, thermohydrogen processing, phase composition, structure, mechanical properties, bulk effect

DOI: 10.3103/S1067821218020062

INTRODUCTION

The development of new titanium alloys with an increased aluminum content and alloys based on titanium aluminides was traditionally considered in view of the creation of highly refractory and heat-resistant materials for the production of important parts of gas-turbine engines [1–7]. Low thermal stability at 500–600°C and insufficient manufacturability under the pressure treatment are some of the main problems when developing alloys with a high volume fraction of the intermetallic α_2-phase—the solid solution based on Ti_3Al aluminide [8, 9]. One promising way to solve these problems to apply hydrogen technologies, in particular, thermohydrogen processing (THP), which is based on the combination of the reversibly hydrogen alloying with the thermal effect [10–14].

However, the fields of using such alloys not associated with the prolonged effect of high temperatures in combination with the oxidative medium, which the problem of the thermal instability of the structure and properties will not be limiting, can turn out to be very promising. One such field is the production of medical wares, in particular, highly loaded implants and surgery tools for orthopedics and traumatology. To fabricate implants, titanium alloys with the normal or lowered elasticity modulus are traditionally used [15–19].

As for medical tools for endoprosthesis operations, their corrosion resistance, hardness, specific strength, wear resistance, and construction rigidity should be considered the main requirements. The latter is determined by the tool geometry and elasticity modulus of the material. It is known that aluminum increases the elasticity modulus of titanium alloys due to an increase in the strength of interatomic bonds in the hcp lattice of titanium. For example, when alloying with aluminum to 10 wt %, the normal elasticity modulus of

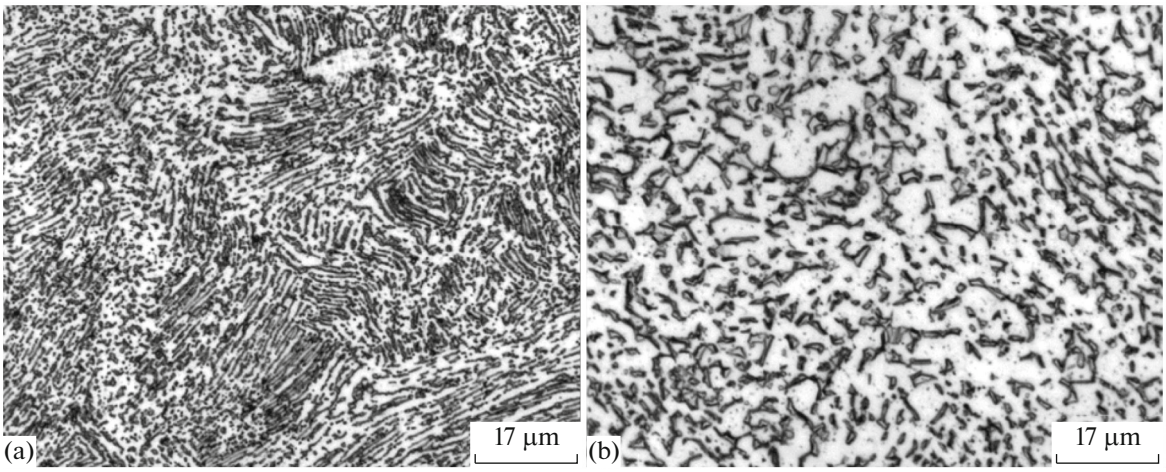

Fig. 1. Structure of the Ti–8.7Al–1.5Zr–2.0Mo alloy (a) in the initial state and (b) after annealing.

α-titanium increases by almost 20% [20]. In view of this, the use of high-modulus titanium alloys with an increased aluminum content is very promising for the fabrication of large-scale orthopedics cutting tools. This will make it possible to fabricate reliable, light, ergonomic, and high-resource surgery tools.

On the other hand, the problems of increasing the fatigue strength, crack resistance, and surface hardness can be successfully solved by applying innovation processing technologies.

The technology including the sequential use of thermohydrogen processing and vacuum ion-plasma nitriding with controlled energy, concentration, and kinetic parameters is one of most promising complex technologies for this group of titanium alloys [21, 22].

The design of process flowsheets and selection of THP modes are based on the construction and analysis of phase composition diagrams of the alloy–hydrogen system and the establishment of regularities of phase and structural transformations in this system under various thermal-kinetic processing parameters [10].

This study is aimed at investigating the influence of hydrogen and thermal effects on the phase composition, structure, and properties of the experimental titanium alloy with a high aluminum content exceeding its solubility limit in α-titanium, as well as the development and approval of THP process flowsheets forming the microcrystalline or bimodal structure.

EXPERIMENTAL

Investigations were performed for the samples cut from the hot-rolled rod 15 mm in diameter of the Ti–8.7Al–1.5Zr–2.0Mo[1] experimental alloy.

[1] Here and below, concentrations of alloying elements and hydrogen are given in wt %.

The experimental party of the rods was fabricated according to the technology accepted for heat-resistant titanium alloys. The aluminum content in the alloy exceeds the solubility limit at the standard temperature in the equilibrium state; therefore, the presence of the ordered α_2-phase should be expected after annealing in its structure (see, for example, [1, 10, 23, 24]). The alloy can be referred to the pseudo-α-class with the Ti_3Al-based intermetallic α_2-phase by the β-stabilization coefficient.

Thermohydrogen processing was performed using a Siverts device (MiTOM, Moscow, 1990) [10] and a Vega-3 vacuum furnace (OOO EFT, Moscow, 2009). SNOL-1,6.2,51/9-I4 laboratory furnaces (NPF TermIKS, Moscow, 2011) were used for the heat treatment (quenching).

The X-ray structural analysis was performed using DRON-4 (NPP Burevestnik, Leningrad, 1989) and DRON-7 (NPP Burevestnik, St. Petersburg, 2009) installations in CuK_α radiation. The microstructure was investigated using a Zeiss Axio-Observer metallographic microscope (Carl Zeiss MicroImaging GmbH, Germany, 2009) with an ImageExpert Pro 3 image analysis system. The mechanical properties under tension were determined according to GOST (State Standard) 1497–84 using a Tiratest-2300 testing machine (Veb Thuringer Industriewerk Rauenstein, Germany, 1990).

RESULTS AND DISCUSSION

In order to equilibrate the alloy, the initial samples were annealed in a vacuum furnace at 950°C for 1 h. The alloy structure in the initial state and after annealing is presented in Fig. 1. Annealing leads to the recrystallization of the initial lamellar alloy structure and to the formation of the structure with a polyhedral α-phase 3–8 μm in size and β-phase spacings along

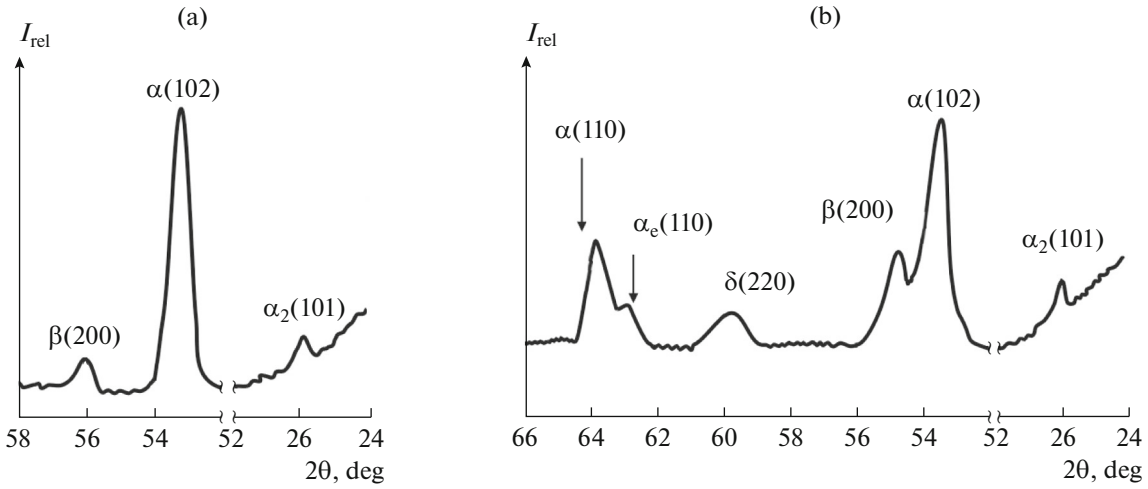

Fig. 2. Fragments of X-ray diffraction patterns of the Ti–8.7Al–1.5Zr–2.0Mo alloy (a) after annealing at 950°C for 1 h and (b) after saturation with hydrogen to a concentration of 0.8%.

the boundaries of α-grains, which is typical of the recrystallized pseudo-α-alloys.

The phase composition of the alloy after annealing is presented by α- and β-phases and a small amount of the α_2-phase (Fig. 2a). The latter was identified by the presence of superstructural reflections of the α_2-phase in the X-ray diffraction pattern at small Bragg angles. The volume fraction of the β-phase determined from the ratio of integrated intensities of reflections (10.2) of the α-phase and (200) reflections of the β-phase was 5–10%.

The samples were saturated with hydrogen at 800°C to concentrations X_H = 0.1, 0.2, 0.4, 0.6, 0.8, and 1.0% with an absolute error up to 0.02%. The hydrogenated samples were cooled with a furnace.

Hydrogen alloying to a concentration of 0.8% does not change the phase composition but leads to an increase in the volume fraction of the β-phase at the standard temperature. For example, the fraction of the β-phase increases to 40–45 vol % at X_H = 0.6%. The partial eutectoid transformation $\beta \rightarrow \alpha_e + \delta$ with the isolation of the hydride δ-phase with a composition close to TiH_2 proceeds in the alloy at a hydrogen content of 0.8% and higher during cooling from the hydrogenation temperature (Fig. 2b). The alloy structure with a hydrogen concentration from 0.8 to 1.0% at the standard temperature consists of β-, α-, and α_2-phases and a eutectoid mixture of α_e- and δ-phases. The amount of eutectoid increases with an increase in the hydrogen content.

To determine the temperature of the $\alpha + \beta/\beta$ transition (A_{c_3}), the phase composition, and the structure of the alloy alloyed with hydrogen at elevated temperatures, the samples were heated to t = 700–1100°C (with intervals of 10–50°C) in a furnace with an air atmosphere and cooled in water after holding for 0.5–2.0 h (depending on the temperature). Heating the samples with the initial hydrogen content to t = 800°C does not lead to a change in the phase composition. When quenching from temperatures of 800°C and above, the α_2-phase is not fixed. This is confirmed by the absence of the superstructural maximum (10.1) in X-ray diffraction patterns, as well as by a decrease in the lattice constant of the α-phase during quenching from 850°C and above (Fig. 3). A decrease in the lattice constant of the α-phase is explained by the fact that the α-matrix is enriched with aluminum during the dissolution of the α_2-phase. Only martensite α' is fixed by quenching from 1100°C, which allows us to determine temperature A_{c_3} for the alloy with the initial hydrogen content as ≈1080°C.

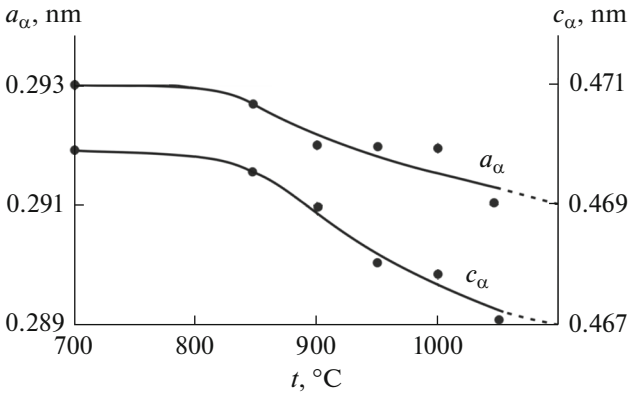

Fig. 3. Temperature dependence of lattice constants of the α-phase of the Ti–8.7Al–1.5Zr–2.0Mo alloy with the initial hydrogen content.

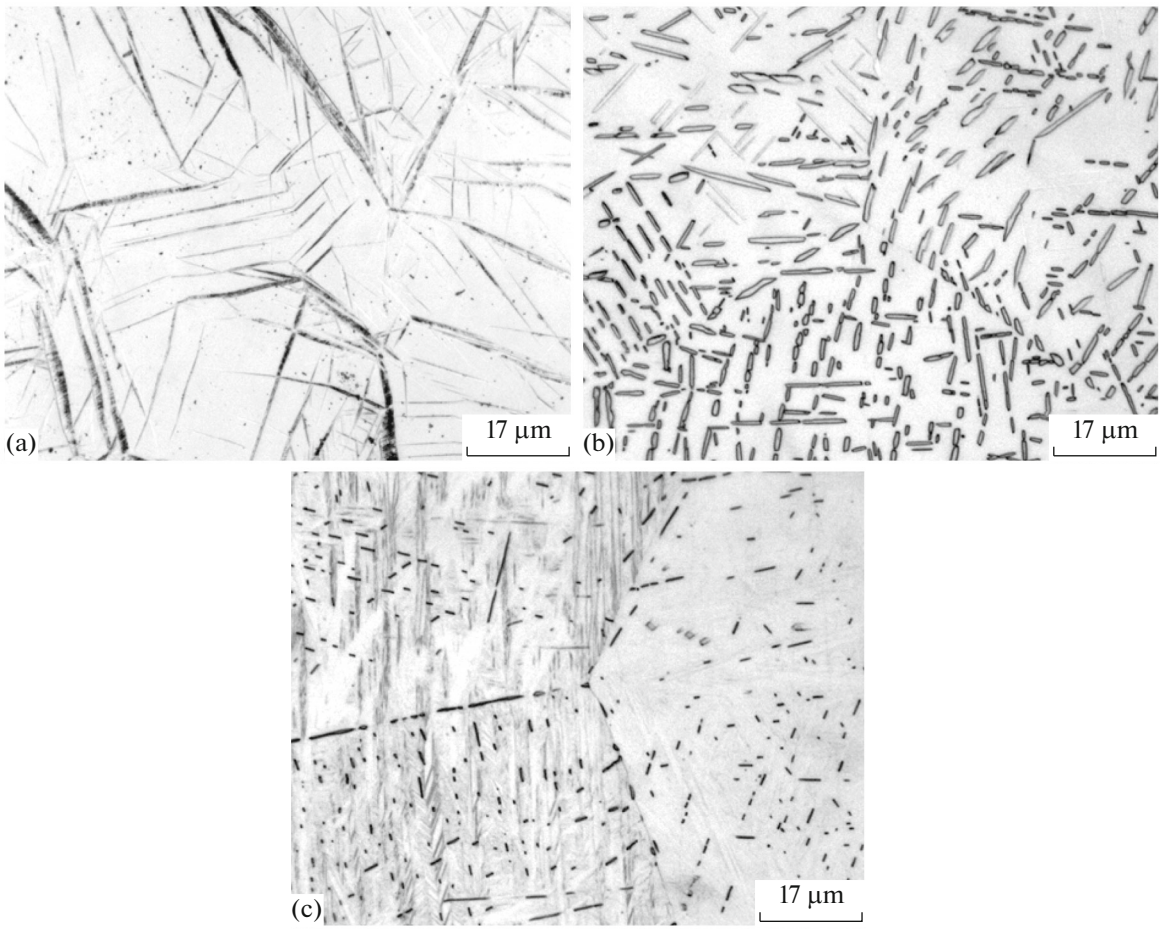

Fig. 4. Microstructure of the Ti–8.7Al–1.5Zr–2.0Mo alloy alloyed with hydrogen and quenched from various temperatures. (a) $X_H = 0.4\%$, $t = 1050°C$; (b) 0.4%, 850°C; and (c) 0.8%, 700°C.

Alloy alloying with hydrogen leads to an increase in the thermodynamic stability of the β-phase, a decrease in the temperature of the $\alpha + \beta \rightarrow \beta$ transition (A_{c_3}), and an increase in the occurrence temperature of the ordered α_2-phase. Temperature A_{c_3} was determined from the data of X-ray diffractometry and a metallographic analysis of quenched samples, notably, from the presence of reflections of the primary α-phase in X-ray diffraction patterns and its particles in the microstructure accurate to ±10°C. Temperature A_{c_3} lowers to 1000°C at a hydrogen concentration of 0.4% and to 870°C at $X_H = 1.0\%$.

When quenching the alloy with a hydrogen content of 0.1% from the β-region, the high-temperature β-phase is subjected to complete martensite transformation, while at hydrogen concentrations from 0.2 to 0.4% it is subjected to the partial martensite transformation $\beta \rightarrow \alpha''$ with the formation of α"- and (β + α")-structures, respectively. The martensite transformation is not implemented during quenching from the β-region at a hydrogen content from 0.6 to 1.0%, and the alloy phase composition is presented only by a metastable β-phase at the standard temperature.

The dissolution temperature of the α_2-phase at $X_H = 0.4\%$ is 850°C, which is 50°C higher than this temperature for the alloy with the initial hydrogen content. An increase in the occurrence temperature of the α_2-phase under alloying with hydrogen is caused by an increase in its disordering stability, which agrees with the data of [23], where the influence of hydrogen on the ordering processes in binary alloys of the Ti–Al system is investigated.

Figure 4 shows the microstructure of the samples of the alloy alloyed with hydrogen after quenching from various temperatures as an example. For example, when quenching the alloy with 0.4% hydrogen from 1050°C (Fig. 4a), martensite transformation $\beta \rightarrow \alpha''$ and the structure $\beta + \alpha''$ with finely lamellar α"-martensite in the β-matrix is formed. When quenching the samples with the same hydrogen content from 850°C, the martensite transformation is suppressed because of the higher hydrogen content in the β-phase [10, 25] and the alloy structure is presented by the particles of the

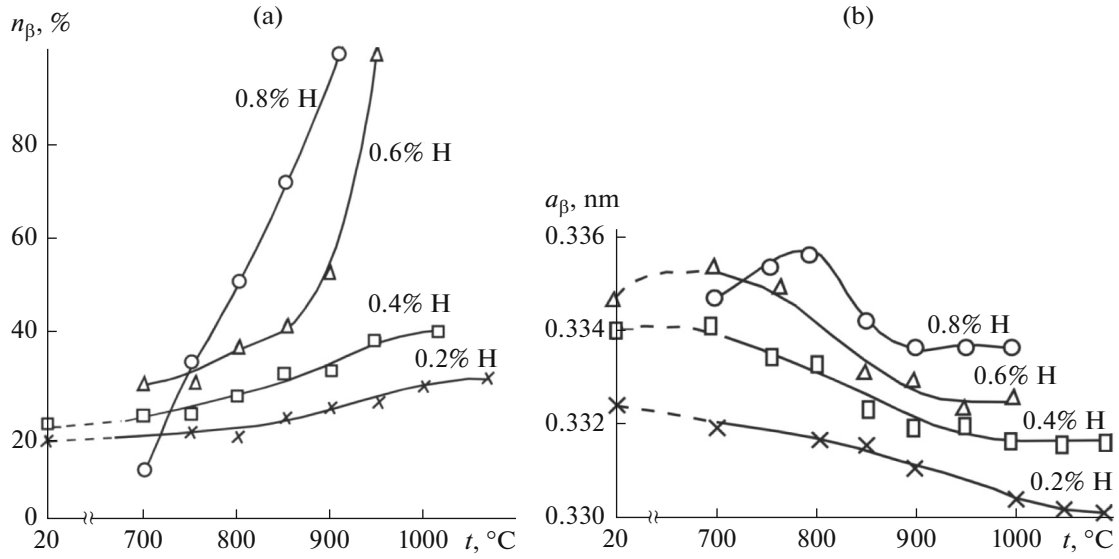

Fig. 5. Influence of the temperature of heating for quenching and hydrogen concentration on (a) the bulk fraction and (b) lattice constant of the β-phase in the Ti–8.7Al–1.5Zr–2.0Mo alloy.

primary α-phase (partially fragmented plates 1–2 μm in thickness) in the body and along the boundaries of the grains of the β-matrix (Fig. 4b).

Figure 5 shows the variation in the volume fraction and lattice constant of the β-phase depending on the heating temperature for quenching. The lattice constant of the β-phase of the samples alloyed with hydrogen to concentrations of 0.1–0.4% decreases with an increase in this temperature, which is caused by an increase in the amount of the β-phase and its depletion with hydrogen.

When quenching the alloy with a hydrogen content of 0.8 and 1.0% from 750°C and below, hydride $\beta \rightarrow \delta$ transformation of the martensite-like shear character occurs. Its causes are apparently the strong enrichment of the β-phase with hydrogen (especially near β/α phase boundaries) and a decrease in its stability with respect to hydride. The hydride phase is isolated in the form of thin plates preferentially near β/α boundaries (Fig. 4c) and is clearly identified in X-ray diffraction patterns. The hydride transformation leads to an abrupt decrease in the amount of the β-phase and its lattice constant because of the hydrogen transfer into the δ-phase (Fig. 5).

The development of the $\beta \rightarrow \delta$ transformation during quenching does not make it possible to determine the temperature-concentration boundary of the occurrence of the hydride phase in the alloy with a hydrogen content from 0.8 to 1.0% by this method. Therefore, we performed high-temperature X-ray investigations for the alloy with $X_H = 0.8$ and 1.0%. The samples were heated in a high-temperature chamber of a DRON-4 diffractometer to temperatures of 200–450°C with an interval of 50°C and X-ray diffraction patterns were recorded at these temperatures. Their analysis showed that the inverse eutectoid transformation in the alloy with $X_H = 0.8$ and 1.0% is finished upon heating at temperatures of 350 and 400°C, respectively, which was determined by the absence of diffraction peaks of the hydride phase in the X-ray diffraction pattern at the recording temperature.

The data on the phase composition of the alloys with various hydrogen contents after quenching from various temperatures are generalized in Table 1. The phases in X-ray diffraction patterns were identified by the presence and location of the following reflections: α-phase—(10.0), (10.1), (10.2), (11.0), (10.3), etc.; β-phase—(200) and (211); hydride δ-phase (TiH_2)—(220); martensite α"-phase–(11.2), (02.2), (11.3), etc.; and ordered α_2-phase—by superstructural reflections (10.1) and (11.0) under the corresponding Bragg angles allowing for the shift of their angular position because of the presence of alloying substitutional elements and hydrogen.

We constructed the diagram of the phase composition of the Ti–8.7Al–1.5Zr–2.0Mo alloy alloyed with hydrogen by the results of our experiments and allowing for classical notions on the formation of the phase composition and structure of titanium alloys under thermal [24] and thermohydrogen [25] treatment (Fig. 6). Its analysis allows us to conclude the following. An increase in the hydrogen concentration from the initial one to 1.0% leads to a decrease in the temperature of the $\beta + \alpha \rightarrow \beta$ transition by 210°C and an increase in the volume fraction of the β-phase at temperatures of the $\beta + \alpha(\alpha_2)$-region. The occurrence temperature in the alloy structure of the α_2-phase increases upon alloying by 50°C. The partial hydride transformation $\beta \rightarrow \delta$ having a shear character is implemented in the alloy with a hydrogen content

Table 1. Phase composition of the Ti–8.7Al–1.5Zr–2.0Mo alloy with various hydrogen contents after quenching

X_H, wt %	Heating temperature for quenching, °C							
	1100	1050	1000	950	900	850	800	≤750
Initial	α'	α + α'	α + α" + β	α + β	α + β	α + β + α_2	α + β + α_2	–
0.1	α"	α + α"	α+α"+β	α + β + (α")	α + β	α + β	α + β + α_2	–
0.2	–	α" + β	α + α" + β	α+β	α + β	α + β	α + β + α_2	–
0.4	–	α" + β	α" + β	α + β	α + β	α + β + α_2	α + β + α_2	–
0.6	–	–	–	β	β	α + β + α_2	α + β + α_2	α + β + α_2
0.8	–	–	–	–	β	α + β + α_2	α + β + α_2	α + β + α_2 + δ
1.0	–	–	–	–	β	α + β + α_2	α + β + α_2	α + β + α_2 + δ

Phases identified by very weak reflections are parenthesized.

above 0.8% during quenching from temperatures below 750°C. The inverse eutectoid transformation α + δ → β upon heating the alloy with 0.8–1.0% hydrogen is finished at temperatures of 350–400°C.

The plotted diagram is the main "tool" for designing the THP process flowsheets of the alloy. When selecting the flowsheet and parameters of hydrogenating (HA) and vacuum (VA) annealing, we should also take into account the change of bulk effects of β → α transformations occurring in the alloy during these operations. Our data on lattice constants of the phases (Figs. 3, 5b) allow us to calculate atomic volumes of phases and bulk effects of transformations according to known relationships [10]. They largely determine the sizes and morphology of α-particles, which are formed due to the β → α isothermal transformation during vacuum annealing at a constant temperature and a continuously decreasing hydrogen content in the alloy and the β-phase, as well as the β → α athermic transformation during cooling after finishing the hydrogenation process [10, 25].

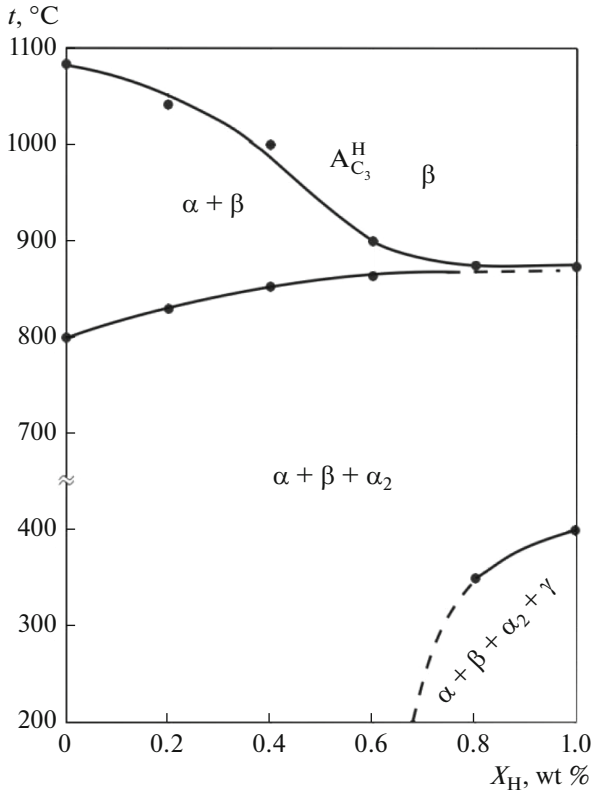

Fig. 6. Temperature-concentration diagram of the phase composition of the Ti–8.7Al–1.5Zr–2.0Mo alloy alloyed with hydrogen.

The atomic volume of the β-phase in the hydrogen-free alloy is larger than the atomic volume of the α-phase. The bulk effect of the β → α transformation (under cooling) is of about 3.5%. Alloying with hydrogen leads to an increase in the atomic volume of the β-phase. An increase in the volume fraction of the β-phase in the (α + β)-region (Fig. 5a) and, correspondingly, a decrease in the fraction of the α-phase determine the rise of the content of the α-stabilizer of aluminum in the latter. This causes a decrease in the atomic volume of the α-phase because aluminum lowers hcp lattice constants of the α-phase. Therefore, an increase in the hydrogen concentration in the alloy should lead to the rise of bulk effects of β → α transformations. Calculations showed that the bulk effects of β → α transformations at 700°C at a hydrogen content in the alloy of 0.1 and 0.6 (0.8)% are 4.5–4.8 and 8.0–8.8, respectively. Large values of the bulk effect of the β → α transformation during alloy degassing lead to high elastic stresses at the coherent boundary of the α-nucleus with the β-matrix and a loss of coherency of this boundary (nucleus "detachment") at early growth stages. The further growth of the α-particle is associated with the diffusion redistribution of main alloying elements between α- and β-phases, which slowly runs at comparatively low temperatures of vacuum annealing (650–700°C), thereby hampering the diffusion growth of α-particles. Thus, nucleation processes of the α-phase dominate over its growth processes with the combination of high bulk effects with a low temperature of the β → α isothermal phase transformation. This leads to the formation of a finely dispersed

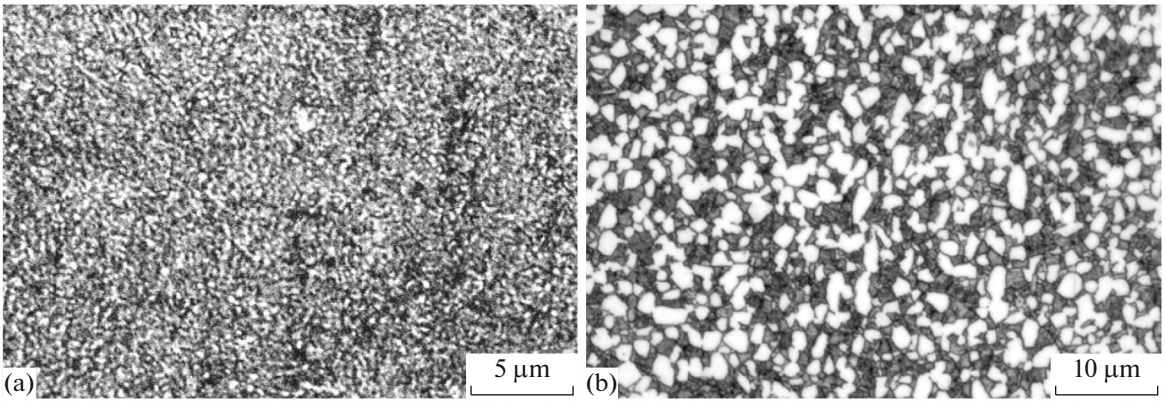

Fig. 7. Structure of the Ti–8.7Al–1.5Zr–2.0Mo alloy after THP according to flowsheets (a) 1 and (b) 2.

"secondary" α-phase with a lamellar morphology [26, 27].

Based on these results, we developed and approved two hydrogenating annealing modes of the Ti–8.7Al–1.5Zr–2.0Mo alloy for samples with sizes of ∅12 × 20 mm:

(i) hydrogenating annealing at t = 880°C to the hydrogen concentration of 0.8% with the subsequent accelerated cooling in a Siverts device ($V_{cool} \approx 1$ K/s) to suppress the eutectoid transformation;

(ii) hydrogenating annealing at t = 900°C with lowering to 800°C to the hydrogen concentration of 0.6% and cooling with the same rate as in the first flowsheet.

The hydrogenation completion corresponded to the β-phase in the first case (Fig. 6), and the alloy phase composition after cooling was presented by only the metastable β-phase. Hydrogenation according to the second flowsheet occurred in the (α + β)-region (Fig. 6), and the alloy structure after cooling contained the primary α-phase, β-phase, and a small amount of the α_2-phase formed in microvolumes of the primary α-phase due to its enrichment with aluminum [26].

Vacuum annealing of the samples hydrogenated according to both flowsheets was performed according to a stepped mode: t = 500°C, τ = 1 h, heating to 680°C, and holding for 7 h. The hydrogen concentration in the samples after vacuum annealing determined by the spectral method using an ISP-51 device (OOO MORS, Troitsk, 2000) was no higher than 0.008%.

The first THP flowsheet was directed to the formation of the finely dispersed alloy structure with a microcrystalline α-phase [10], and the second one was directed to the formation of a bimodal structure with a globular primary α(α_2)-phase and finely dispersed secondary α-phase in the β-matrix. Alloy microstructures after the THP according to the described flowsheets and modes are presented in Fig. 7.

The analysis of structures shows that processing according to the first flowsheet gives a structure with a finely dispersed α-phase in the bulk of β-grains without the α-bordering (Fig. 7a). The second THP flowsheet forms a bimodal structure with a globular α(α_2)-phase with sizes of 2–5 μm and a finely dispersed mixture of α- and β-phases (Fig. 7b). Similar structures were resulted, for example, in [13, 27] from the THP with low-temperature (650–700°C) vacuum annealing. Billets of cylindrical samples for tensile tests were processed according to these modes. The results of tests are presented in Table 2.

Table 2. Mechanical properties of the Ti–8.7Al–1.5Zr–2.0Mo after the THP

Processing mode	Mechanical properties				
	σ_u, MPa	$\sigma_{0.2}$, MPa	δ, %	ψ, %	*HRC*
THP-1 HA: t = 880°C, X_H = 0.8%; VA: t = 500°C, 1 h + 680°C, 7 h	1100	1060	4	9	43
THP-2 HA: t = 900 → 800°C, X_H = 0.6%; VA: t = 500°C, 1 h + 680°C, 7 h	1080	1020	11	25	38
Annealing t = 950°C, 1 h	1020	960	14	30	32

An analysis of mechanical properties showed that the THP according to both modes leads to an increase in strength characteristics and hardness. However, plasticity indices fall, especially when applying mode 1.

CONCLUSIONS

(i) The influence of alloying with hydrogen and heat treatment on the phase composition and structure of the Ti–8.7Al–1.5Zr–2.0Mo experimental titanium alloy is established experimentally. It is shown that a single-phased β-structure is fixed by quenching from the β-region with the concentration of introduced hydrogen of 0.6% and higher. Saturation with hydrogen to 0.8–1.0% leads to the implementation of the shear hydride transformation $\beta \rightarrow \delta$ during quenching from temperatures below 750°C and to partial eutectoid transformation $\beta \rightarrow \alpha + \delta$.

(ii) The temperature-concentration diagram of the phase composition of the alloy–hydrogen system is constructed. It is established that hydrogen extends the stability region of the β-phase, lowering the temperature of the $\beta/\alpha + \beta$ transition by 210°C (at X_H = 1.0%), and increases the occurrence temperature of the ordered α_2-phase by 50°C.

(iii) Process flowsheets and thermohydrogen processing modes are developed and approved for alloy samples. Mechanical characteristics of alloy samples are determined. It is established that the THP leads to an increase in strength and hardness when compared with the annealed state.

REFERENCES

1. Pol'kin, I.S., Kolachev, B.A., and Il'in A.A., Titanium aluminides alloys based on them, *Tekhnol. Llegk. Splav.*, 1997, no. 3, pp. 32–39.
2. Nochovnaya, N.A. and Ivanov, V.I., Intermetallic compounds based on titanium. Analysis of the state of the question, *Titan*, 2007, no. 1, pp. 44–48.
3. Lutjering, G., Proske, G., and Terlinde, G., Influence of microstracture, texture and environment on tensile properties of super alpha 2, in: *Titanium-95. Science and Technology*: Proc. 8th World Conf. on Titanium, Birmingham: Institute of Materials, 1996, vol. 1, pp. 332–339.
4. Egry, I., Brooks, R., Holland-Mozitz, D., Novakovic, R., Matsushita, T., Ricci, E., Seetharaman, S., and Wunderlich, R., Temperophysical properties of titanium aluminides, in: *Ti-2007. Science and Technology*: *Proc. 11th World Conf. on Titanium*, Kyoto: The Japan Institute of Metals, 2007, vol. 1, pp. 671–674.
5. Roth-Fagaraseanu, D. and Appel, F., TiAl—new opportunity in the aerospace industry, in: *Ti-2003. Science and Technology*: *Proc. 10th World Conf. on Titanium*, Hamburg: Wiley, 2003, vol. 5, pp. 2899–2907.
6. Hervier, Z., Belaygue, P., Alexis, J., Petit, J.-A., and Uginet, J.-F., Titanium alloys for high temperature applications, in: *Ti-2007. Science and Technology*: *Proc. 11th World Conf. on Titanium*, Kyoto: The Japan Institute of Metals, 2007, vol. 2, pp. 1349–1353.
7. Heritier, P., Titanium for high strength aerospace forgings, in: *Ti-2007. Science and Technology*: *Proc. 11ht World Conf. on Titanium*, Kyoto: The Japan Institute of Metals, 2007, vol. 2, pp. 1313–1317.
8. Wang Bin, Jia Tiancong, and Zou Dunxue, A study on long-term stability of Ti_3Al–Nb–V–Mo alloy, *Mater. Sci. Eng. A*, 1992, vol. 153, nos. 1–2, pp. 422–426.
9. Froes, F.H., Suryanarayana, C., and Eliezer, D., Production, characteristics and commercialization of titanium aluminides, *ISIJ Int.*, 1991, vol. 31, no. 10, pp. 1235–1247.
10. Il'in, A.A., Kolachev, B.A., Nosov, V.K., and Mamonov, A.M., *Vodorodnaya tekhnologiya titanovykh splavov* (Hydrogen Technology of Titanium Alloys), Moscow: MISIS, 2002.
11. Senkov, O.N. and Jonas, J.J., Solute softening of alpha titanium—hydrogen alloys, in: *Advances in the science and technology of titanium alloy processing*: *Proc. Int. Symp.*, Anaheim, CA: TMS, 1996, pp. 109–116.
12. Ilyin, A.A., Polkin, I.S., Mamonov, A.M., and Nosov, V.K., Thermohydrogen treatment—base of hydrogen treatment of titanium alloys, in: *Titanium-95. Science and Technology*: *Proc. 8th World Conf. on Titanium*, Birmingham: Institute of Materials, 1996, pp. 2462–2469.
13. Ilyin, A.A., Mamonov, and A.M., Kusakina, Y.N., Thermohydrogen treatment of shape casted titanium alloys, in: *Advances in the science and technology of titanium processing*: *Proc. Int. Symp.*, Anaheim, CA: TMS, pp. 639–646.
14. Apgar, L.S., Yolton, C.I., and Sagib, M., Microstructure and property modification of vCast alpha-2 titanium alloys by thermochemical processing with hydrogen, in: *Titanium-92. Science and Technology*: *Proc. 7th World Titanium Conf.*, San-Diego, CA; Warrendale, PA: Minerals, Metals and Materials Society, 1993, vol. 2, pp. 1331–1335.
15. Niinomi, M., Titanium alloys for biomedical, dental and healthcare Applications, in: *Ti-2007. Science and Technology*: *Proc. 11th World Conf. on Titanium*, Kyoto: The Japan Institute of Metals, 2007, vol. 2, pp. 1417–1425.
16. Tahara, M., Kim, H.Y., Inamura, T., Hosoda, H., and Miyazaki, S., Effect of addition on mechanical properties of Ti–20Nb–4Zr–2Ta (at %) biomedical superelastic alloy, in: *Ti-2007. Science and Technology: Proc. 11th World Conf. on Titanium*, Kyoto: The Japan Institute of Metals, 2007, vol. 2, pp. 1453–1454.
17. Jelliti Sami, Richrd Caroline, Retraint Delphine, Demangel Clemence, and Landoulsi Jessem, Surface modification of low-modulus Ti35NbXZr alloys with nanotube arrays, in: *Ti-2011: Proc. 12th World Conf. on Titanium*, Beijing: The Japan Institute of Metals, 2011, vol. 3, pp. 2042–2046.
18. Dongyan Ding, Hegang Liu, Congqin Ning, and Zhaohui Li, Development of biomedical Ti–Cr alloys with changeable Young's modulus via deformation-induced transformation, in: *Ti-2011: Proc. 12th World Conf. on Titanium*, Beijing: The Japan Institute of Metals, 2011, vol. 3, pp. 2046–2050.

19. Mi Gong, Minjie Lai, Bin Tang, Hongchao Kou, and Jinshan Li, Lian Zhou, Young's modulus of Ti–Cr–Sn–Zr alloys with meta-stable beta phase, in: *Ti-2011: Proc. 12th World Conf. on Titanium*, Beijing: The Japan Institute of Metals, 2011, vol. 3, pp. 2180–2184.

20. Collings, E.W., *The Physical Metallurgy of Titanium Alloys*, ASM International (OH), 1984.

21. Mamonov, A.M., Skvortsova, S.V., and Spektor, V.S., Principles of construction of complex technological processes for the production of implants made of titanium alloys including vacuum ion-plasma nanotechnologies, *Titan*, 2012, no. 3, pp. 45–50.

22. Itoh, Y., Itoh, A., Azuma, H., and Hioki, T., Improving the tribological properties of Ti–6Al–4V alloy by nitrogen-ion implantation, *Surf Coat. Technol.*, 1999, vol. 111, pp. 172–176.

23. Belov, S.P., Il'in, A.A., Mamonov, A.M., and Aleksandrova, A.V., Theoretical analysis of ordering processes in an alloy based on Ti_3Al. The influence of hydrogen on stability of the Ti_3Al intermetallic compound, *Metally*, 1994, no. 2, pp. 76–80.

24. Kolachev, B.A., Elagin, V.I., and Livanov, V.A., *Metallovedenie i termicheskaya obrabotka tsvetnykh metallov i splavov* (Metallurgy and Thermal Processing of Nonferrous Metals and Alloys), Moscow: MISIS, 2005.

25. Il'in, A.A., *Mekhanizm i kinetika fazovykh i strukturnykh prevrashchenii v titanovykh splavakh* (Mechanism and Kinetics of Phase and Structural Transformations in Titanium Alloys), Moscow: Nauka, 1994.

26. Mamonov, A.M., Kusakina, Yu.N., and Il'in, A.A., Regularities of phase composition and structure formation in heat-resistant titanium alloy with intermetallic hardening at hydrogen alloying, *Metally*, 1999, no. 3, pp. 84–87.

27. Mamonov, A.M., Skvortsova, S.V., Agarkova, E.O., and Umarova, O.Z., Physicochemical and technological principles of thermo-stable bimodal structure type formation in heat-resistant titanium alloys and titanium aluminide based alloys at reversible hydrogen alloying, *Titan*, 2013, no. 3, pp. 9–16.

Translated by N. Korovin